RESEARCH ARTICLE

Impact of Nanoethosomes Loaded with Polyherbal Extracts on the Mechanisms Involved in Wound Healing *In-vitro* Research

Mekala K, Shaheedha SM*, Prakash R

Crescent School of Pharmacy, B. S. Abdur Rahman Crescent Institute of Science and Technology, Vandalur, Chennai, Tamilnadu, India

Received: 24th January, 2024; Revised: 24th April, 2024; Accepted: 16th May, 2024; Available Online: 25th September, 2024

ABSTRACT

This study focuses on formulating and optimizing Polyherbal Nanoethosomes for controlled drug delivery, utilizing a polyherbal extract comprising *Basella alba* L., *Portulaca oleracea* L., *Lawsonia inermis* L., *Trigonella foenum* L., and *Peristrophe paniculata* L. Comprehensive characterization revealed a variety of secondary metabolites within the extract. The primary goal was to create poly herbal extract-entrapped ethosomes that could be integrated into a sustained-release transdermal gel dosage. We prepared nanoethosomes using phosphatidylcholine, ethanol, Tween 80, and SLS, and optimized them using Design Expert software. The characteristics included size (particle size: 121 ± 2.60 nm) and entrapment efficiency (81.91 ± 1.92%), followed by incorporation into a carbopol gel for skin application. We performed *in-vitro* permeation studies and cytotoxic assays on L-929 cells, which revealed favorable outcomes. Optimized nanoethosomes displayed desirable particle characteristics, highlighting their potential for controlled drug delivery. The nano vesicular gels had good rheological and physical properties (polydispersity index: 0.41 ± 0.04, zeta potential: -8.12 ± 1.25 mV), which meant they could be used topically. This research underscores the compatibility of plant extracts with formulation components, offering a foundation for Polyherbal Nanoethosomes in pharmaceutical formulations. The study emphasizes precise control over particle attributes and suggests potential applications in enhancing drug release and bioavailability.

Keywords: Polyherbal nanoethosomes, Controlled drug delivery, Transdermal gel, optimization.

International Journal of Drug Delivery Technology (2024); DOI: 10.25258/ijddt.14.3.12

How to cite this article: Mekala K, Shaheedha SM, Prakash R. Impact of Nanoethosomes Loaded with Polyherbal Extracts on the Mechanisms Involved in Wound Healing *In-vitro* Research. International Journal of Drug Delivery Technology. 2024;14(3):1334-1343.

Source of support: Nil.

Conflict of interest: None

INTRODUCTION

Burn injuries represent a significant global public health challenge, inflicting considerable morbidity and mortality while posing substantial burdens on healthcare systems.[1] Effective management of these wounds is crucial to minimize complications, facilitate tissue regeneration, and improve patient outcomes. While various treatment modalities, including surgical interventions, topical therapies, and supportive care, are available, there remains an ongoing quest for innovative approaches to enhance the healing process and mitigate associated sequelae.

In recent years, there has been a burgeoning interest in harnessing the therapeutic potential of natural compounds for wound healing, driven by their diverse pharmacological properties and relatively favorable safety profiles.[2] Among these natural remedies, botanical products have garnered particular attention for their ability to modulate inflammatory responses, promote tissue regeneration, and combat microbial colonization.[3] However, translating botanical therapies into clinically viable treatments requires the development of effective delivery systems capable of optimizing drug bioavailability and target tissue localization.

Nanoethosomes, nanosized liposomal carriers, have emerged as a promising platform for delivering bioactive compounds due to their ability to encapsulate both hydrophilic and lipophilic agents, thereby enhancing their solubility, stability, and therapeutic efficacy.[4] In the context of burn wound management, nanoethosomes offer unique advantages, including deep tissue penetration, sustained drug release, and minimizing systemic side effects.[5] Nevertheless, the application of nanoethosomal delivery systems in burn care remains relatively unexplored, highlighting a critical gap in current research efforts.

Moreover, traditional burn treatments often prove inadequate in addressing the multifaceted nature of burn injuries, underscoring a scarcity of studies focusing on the

*Author for Correspondence: mekala2016mmc@gmail.com

development of novel therapeutic interventions, especially in regions like the United Kingdom.[6] This underscores the urgent need for innovative approaches to burn wound management that amalgamates evidence-based medicine with emerging technologies and natural remedies.

To address these pressing challenges, the present study endeavors to formulate and evaluate a polyherbal nanoethogel aimed at expediting burn wound healing. Drawing upon the synergistic properties of multiple botanical extracts, the nanoethogel is meticulously designed to enhance tissue regeneration, alleviate inflammation, and prevent infection. Through a comprehensive assessment of its efficacy in both *in-vitro* and *in-vivo* models, this research aims to advance our understanding of the therapeutic potential of polyherbal formulations in burn care and lay the groundwork for their clinical translation.

Renowned for their ability to activate mitogen-activated protein and promote angiogenesis *in-vitro*, fibroblasts, endothelial cells, smooth muscle cells, and dendritic epidermal T-cells release keratinocyte growth factor (KGF), a paracrine growth factor.[5] Natural botanical products play a significant role in fibroblast and keratinocyte proliferation.[6] These products include growth factors, cell signaling molecules, and adhesion molecules.[7,8] The realm of nanotechnology holds tremendous potential for advancing herbal medicine science, facilitating the detection, development, and delivery of interventions to bolster health and mitigate disease risks. This exposition aims to elucidate these advances and underscore the potential benefits of nanomaterials, albeit with the requisite acknowledgment of potential health concerns associated with nanoparticles. Various prior investigations have alluded to the antibacterial, antifungal, and antitumor attributes of *Lawsonia inermis*.[9] Over time, traditional plant-based medicines have emerged as a natural avenue for addressing diverse human ailments. Herbal drugs typically constitute individual plant extracts or fractions thereof or combinations thereof from disparate botanical sources.[10] Contemporary scientific discourse has evinced heightened interest in harnessing naturally occurring, biologically active compounds of medicinal relevance.[11] Literature scrutiny underscores the antifungal,[12] opioid analgesic and anti-inflammatory properties of *Basella alba* leaves.[13] Moreover, *B. alba* has demonstrated commendable anti-inflammatory and antibacterial characteristics.[14] These botanical attributes lay the foundation for potential wound-healing efficacy. By bridging the gap between traditional medicine, nanotechnology, and modern wound care practices, this study strives to contribute to the development of safe, effective, and accessible therapies for burn injuries, ultimately improving patient outcomes and raising healthcare standards.

MATERIALS AND METHODS

The study employed a systematic approach to develop and evaluate a polyherbal nanoethosomal topical gel aimed at enhancing bioavailability for burn wound healing. Key materials, including phosphatidylcholine, ethanol, Tween 80, and SLS were sourced from M/S Sigma Aldrich, USA. Plant extracts from *B. alba* L., *Portulaca oleracea* L., *L. inermis* L., *Trigonella foenum* L., and *Peristrophe paniculata* L. were collected, authenticated, and subjected to extraction using 70% ethanol through maceration, followed by concentration and storage. Phytochemical quantification involved spectrophotometric assays for flavonoids, phenolic compounds, tannins, and alkaloids, with results expressed as mg per gram of plant extract.[15] Pre-formulation studies focused on drug-excipient compatibility using fourier transform infrared spectroscopy (FTIR) and optimization of nanoethosomes via factorial design using Design Expert software.[16] Characterization of nanoethosomes included morphological analysis using optical microscopy and SEM (scanning electron microscopy), as well as determination of vesicle size, surface charge, and entrapment efficiency using dynamic light scattering (DLS) and ultracentrifugation.[17] *In-vitro* permeation studies assessed skin permeation parameters through modified Franz diffusion cells, while cytotoxicity assays using the MTT assay evaluated cell viability and IC_{50} values.[18] Live cell assays and DAPI (4',6-diamidino-2-phenylindole) staining assays were conducted to assess cytotoxic and nuclear effects. Furthermore, nanovesicular ethosome gels were formulated using Carbopol, with evaluations performed for visual appearance, pH, viscosity, and extrudability. Statistical analysis was conducted using Design-Expert software, with data presented as mean ± SD and significance determined through Student t-tests ($p < 0.05$).

RESULTS

Phytochemicals Analysis

The polyherbal sample exhibited the presence of various secondary metabolites based on the conducted phytochemical tests. Tannins, flavonoids, phenols, saponins, alkaloids, terpenoids, carbohydrates, and steroids were detected in the sample. Additionally, glycosides were identified, indicating a diverse array of bioactive compounds in the polyherbal formulation. However, reducing sugars were found to be absent in the tested sample. This comprehensive profile of secondary metabolites suggests the potential therapeutic and pharmacological significance of the polyherbal formulation.

Quantification of phenolic and tannin contents

The phytochemical composition of five plant species, namely *T. foenum, B. alba, L. inermis, P. oleracea,* and *P. paniculata,* was analyzed, revealing distinct profiles of tannin, flavonoid, phenolic, and alkaloid content. Trigonella exhibited the highest levels of tannin (86.55 ± 0.13), while *P. oleracea* demonstrated elevated alkaloid content (49.17 ± 0.50). *B. alba* displayed substantial levels of flavonoids (58.18 ± 0.30) and phenolics (132.13 ± 0.09), whereas *Lawsonia* exhibited comparatively lower concentrations across all categories. *P. paniculata* showcased notable phenolic content (151.22 ± 0.28) but relatively lower alkaloid levels (13.12 ± 0.23). These findings underscore the diverse phytochemical profiles among the studied plant species, providing valuable insights into their potential medicinal and nutritional properties (Table 1 and Figure 1).

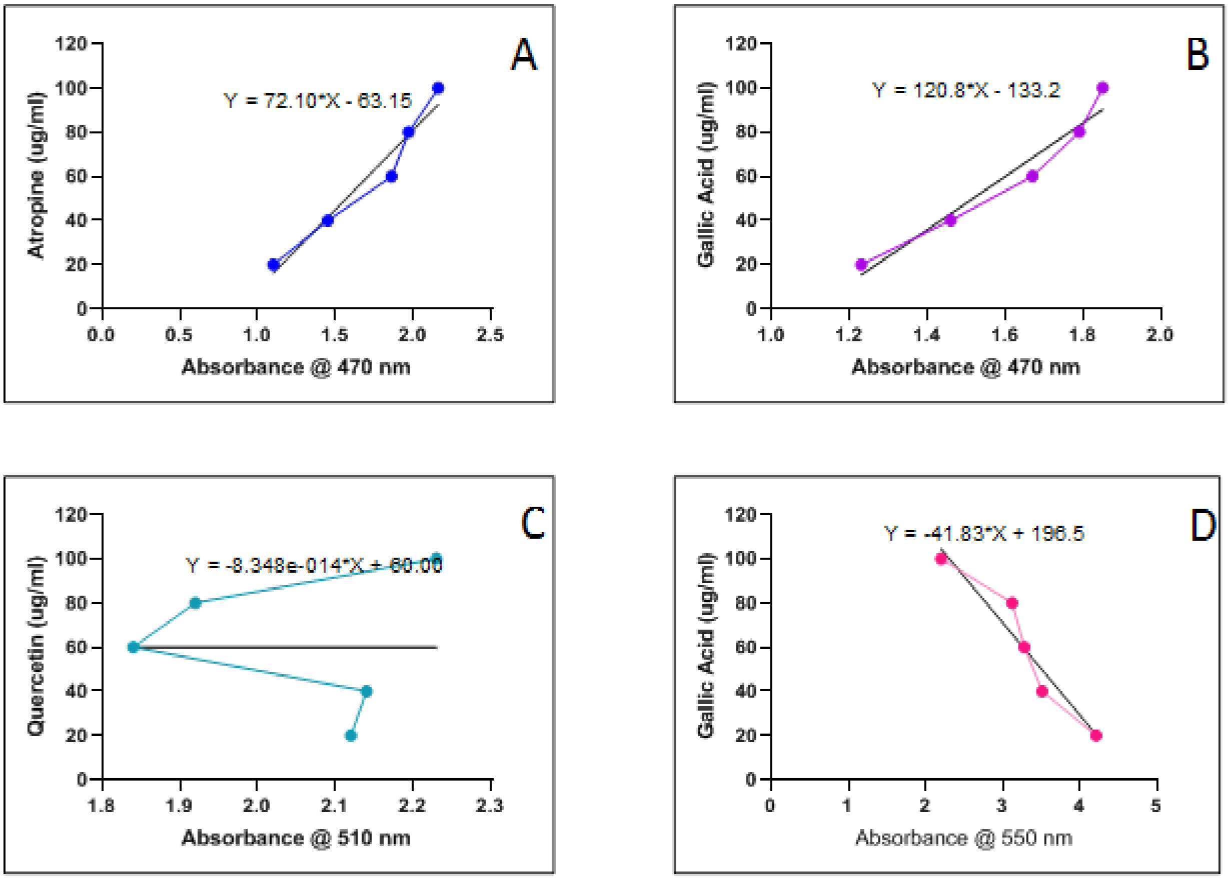

Figure 1: Quantification of phytochemicals standard curve (A). Alkaloids, (B) Tannins, (C) Flavonoids, (D) Phenolic compounds

Table 1: Quantitative analysis of polyherbal extracts

Polyherbal extract	*Tannin*	*Flavanoid*	*Phenolic*	*Alkaloid*
T. foenum	86.55 ± 0.13	59.77 ± 0.41	147.21 ± 0.09	49.17 ± 0.50
B. alba	72.92 ± 0.13	58.18 ± 0.30	132.13 ± 0.09	23.69 ± 0.15
L. inermis	29.82 ± 0.09	55.10 ± 0.48	116.01 ± 0.10	18.50 ± 0.21
P. oleracea	99.51 ± 0.10	51.15 ± 0.37	141.98 ± 0.22	26.10 ± 0.26
P. paniculata	77.25 ± 0.14	55.85 ± 0.20	151.22 ± 0.28	13.12 ± 0.23

Mean ± standard deviation (SD) based on triplicate measurements (n=3). Tannin, Flavanoid, Phenolic, and Alkaloid content are presented in milligrams per gram (mg/g) dry weight.

FTIR analysis

The FTIR spectrum of plant extracts displayed characteristic peaks, such as a sharp peak at 3000-2970 cm^{-1} indicating phenolic OH group presence, and a strong peak around 1600 cm^{-1} attributed to mixed vibrations of (C=C) and (C=O). Peaks at 1300 to 1200 cm^{-1} represented C-H bending vibrations, while those below 1000 cm^{-1} indicated trans C-H vibrations. These features hinted at the plant extracts' composition and potential medicinal phytochemicals. In the drug-excipient compatibility study, investigating interactions between plant extracts and key excipients (Phosphatidylcholine, SLS, Tween 80), the FTIR spectra of the mixture revealed no significant interaction. Major characteristic peaks of plant extracts remained, affirming the compatibility of the nano-vesicular system formulation and preserving the phytochemical integrity of the plant extractsshowed in Figure 2 (A-C).

Optimization of nanoethosomes

The formulations of nanoethosomes were systematically characterized to assess their key physicochemical properties. The vesicle size of the formulations ranged from 110 ± 3.54 nm (EH1) to 265 ± 3.84 nm (EH9), indicating a controlled and tunable size distribution. The zeta potential, a measure of surface charge, exhibited variations from 5.13 ± 1.05 mV (EH1) to -20.18 ± 1.09 mV (EH9), suggesting a surface charge suitable for stability. Entrapment efficiency, a crucial parameter for drug delivery systems, demonstrated high values ranging from 65.13 ± 1.50% (EH1) to 94.93 ± 3.17% (EH9), indicating effective encapsulation of bioactive compounds within the nanoethosomes. The polydispersity index, a measure of the size distribution uniformity, showed values between 0.27 ± 0.04 (EH9) and 0.51 ± 0.06 (EH1), suggesting a relatively narrow and consistent size distribution across the formulations which is shown in Table 2. Overall, these results underscore the successful optimization of nanoethosome synthesis, achieving desired vesicle sizes, surface charges, and encapsulation efficiencies. Such tailored formulations hold promise for effective and controlled drug delivery applications, emphasizing their potential significance in pharmaceutical and biomedical research. Optimizing the formulation of nanoethosomes involved a systematic variation in the concentrations of SNS (sodium taurocholate), Tween 80, ethanol, and phosphatidylcholine (PC) in milligrams, as depicted in Figure 3 A-D. In contrast, Figure 3E displays a response surface model depicting the factors affecting nanoethosome vesicle size, while Figure 3F illustrates a similar model for the entrapment efficiency of phytochemicals in nanoethosomes.

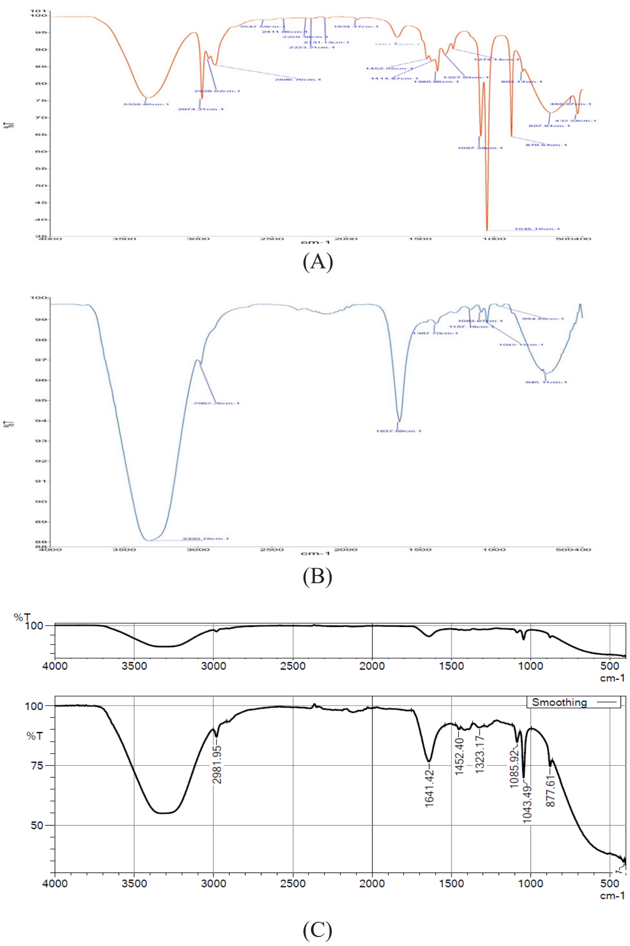

Figure 2: FTIR Spectrum analysis of drug excipients (A- Phosphatidyl choline; B- SLS; (c) FTIR spectrum of plant extracts and excipients with the wavelength ranging from 400-4000 cm^{-1})

Nanoethosome characterization

Optical Microscopy Analysis

The optical microscopy analysis of ethosome formulations (EH2, EH6, EH9) revealed distinct vesicle features. EH2 exhibited a

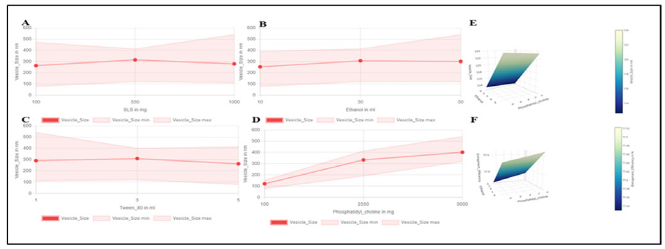

Figure 3: Optimization of drug excipients for nano ethosomal vesicle size in Design expert Software, SLS (A), Ethanol (B), Tween 80 (C) and phosphatidylcholine (D). Surface plot model was illustrated with Entrapment efficiency and vesicle size in ethosomes optimization (E&F)

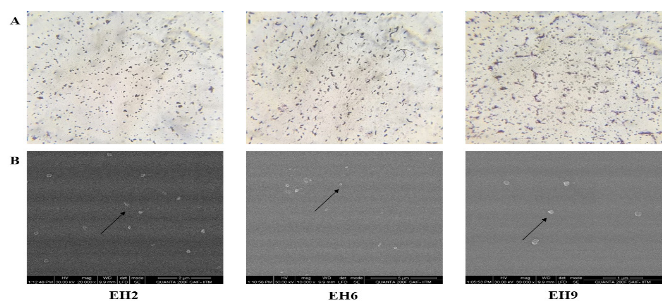

Figure 4: Characterization of selected nanoethosomes in optical microscope at the magnification of 60X (A) and high-resolution scanning electron microscopic images of nano ethosomes at the magnification of 50000X (B)

Table 2: Nanoethosome formulation characteristics

Formulations	*Vesicle size (nm)*	*Zeta potential (mV)*	*Entrapment efficiency (%)*	*Polydispersity index*
EH1	110 ± 3.54	5.13 ± 1.05	65.13 ± 1.50	0.51 ± 0.06
EH2	121 ± 2.60	-8.12 ± 1.25	81.91 ± 1.92	0.41 ± 0.04
EH3	131 + 4.10	-7.92 ± 2.18	82.60 ± 3.13	0.50 ± 0.02
EH4	170 ± 6.01	-8.91 ± 1.08	80.12 ± 3.0	0.49 ± 0.07
EH5	193 ± 1.38	-9.15 ± 1.53	85.35 ± 2.50	0.31 ± 0.08
EH6	239 ± 1.91	-11.97 ± 2.82	92.15 ± 2.62	0.29 ± 0.05
EH7	247 ± 5.10	-13.76 ± 1.81	91.12 ± 1.60	0.41 ± 0.03
EH8	250 ± 3.81	-15.39 ± 1.50	90.18 ± 3.10	0.35 ± 0.05
EH9	265 ± 3.84	-20.18 ± 1.09	94.93 ± 3.17	0.27 ± 0.04

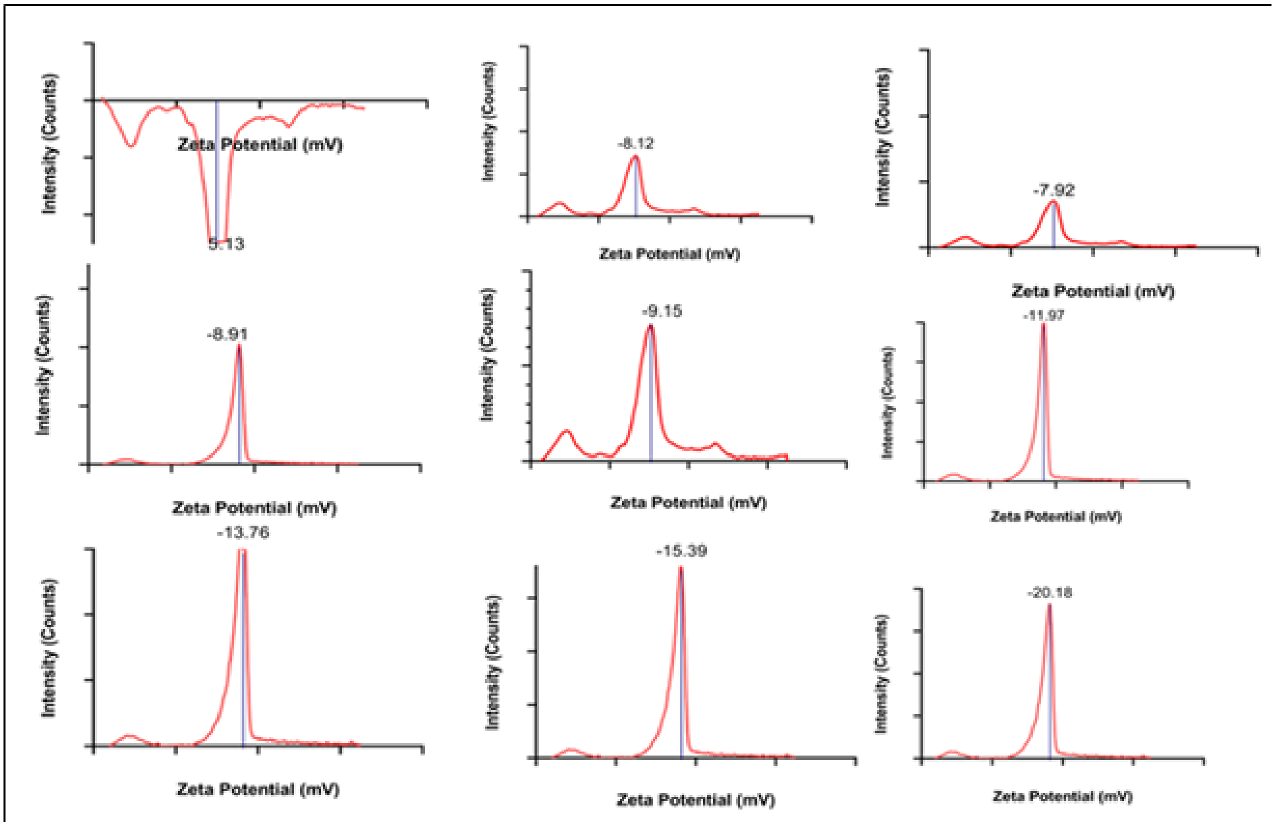

Figure 5: Zeta potential

spherical and elevated shape, EH6 displayed a spherical and busted appearance, while EH9 showed an uneven, spherical morphology, as observed at a 20-X magnification using an ACCUSCOPE inverted microscope shown in Figure 4 (A&B). and zeta potential in Figure 5.

SEM Characterization

SEM analysis at 50000X magnification provided further insights into the surface morphology and vesicle size of the Ethosome formulations. EH2 demonstrated a vesicle size of 121 nm with a spherical and elevated morphology. EH6, with a vesicle size of 239 nm, exhibited a spherical and busted appearance, while EH9, with a vesicle size of 265 nm, displayed uneven spherical characteristics, which are shown in Table 2 and Figure 5. Among the studied ethosome formulations (E2, E6, E9), overall, E2, E6, and E9 demonstrated superior results in terms of vesicle morphology and size. Notably, E2, E6, and E9 displayed characteristics such as elevated, spherical, and uneven spherical morphologies, respectively, indicating promising attributes for potential applications in drug delivery.

Data are presented as mean ± standard deviation (SD) (n = 3). Vesicle size is expressed in nanometers (nm), zeta potential in millivolts (mV), entrapment efficiency in percentage (%), and polydispersity index is dimensionless.

***In-vitro* permeation studies**

The permeation characteristics of phytochemical formulations through cellulose and nylon membranes with 0.45 and 0.22 µm pore sizes were investigated. In the case of cellulose 0.45 µm formulations, cumulative amounts permeated ranged from 30.13 to 112.54 µL/cm^2, with corresponding permeation flux values of 0.98 to 2.45 µL/cm^2/h. The permeability coefficients (Kp) varied from 0.00135 to 0.00519 cm/h, and enhancement ratios (ER) ranged from 0.65 to 2.56, demonstrating the impact of formulation on permeation. For nylon 0.45 µm and both cellulose and nylon 0.22 µm formulations, similar trends in permeation parameters were observed, with differences attributed to membrane characteristics. Overall, the study provides insights into the permeation behavior of phytochemical formulations through different membranes, aiding in the optimization of delivery systems, which is shown in Table 3.

***In-vitro* studies of polyherbal nanoformulations (EH2) in L-929 cell lines**

Cytotoxicity assay (MTT Assay)

A phase contrast microscope was used to assess cell morphology in order to validate the results of the MTT experiment. By assessing the morphological alterations associated with apoptosis, cell morphology evaluation offers a qualitative evaluation of the healing effects of polyherbal extracts and their nano vesicular formulations, shown in Figure 6(A). A cell that is going through apoptosis or dying exhibits morphological changes, such as shrinking, rounded edges, and separation from other cells. Phase contrast microscopy

Table 3: Permeation parameters of phytochemical formulations through cellulose and nylon membranes A) 0.45 µm B) 0.22 µm

A.Formulation (Cellulose 0.45 µm)	*Cumulative amount permeated µL/cm^2*	*Permeation flux (J) (µL/cm^2/h)*	*Permeability coefficient (Kp) (cm/h)*	*Enhancement ratio*	*Amount deposited (µL/cm^2)*
EH1	30.13 ± 2.47	0.98 ± 0.07	0.00135	0.65	16.67 ± 0.20
EH2	51.45 ± 3.14	1.12 ± 0.04	0.00274	1.25	12.46 ± 0.23
EH3	49.14 ± 7.21	1.01 ± 0.02	0.00153	0.75	14.57 ± 0.45
EH4	57.12 ± 4.71	1.14 ± 0.05	0.00163	0.81	15.60 ± 0.30
EH5	66.37 ± 4.70	1.47 ± 0.12	0.00205	1.20	18.88 ± 0.15
EH6	89.85 ± 1.32	1.89 ± 0.19	0.00394	1.54	11.78 ± 0.14
EH7	81.01 ± 3.50	1.63 ± 0.02	0.00295	1.26	12.67 ± 0.13
EH8	90.39 ± 4.16	1.98 ± 0.03	0.00318	1.59	15.67 ± 0.45
EH9	112.54 ± 2.45	2.45 ± 0.02	0.00519	2.56	15.78 ± 0.16
Formulation (Nylon 0.45 µm)					
EH1	50.13 ± 3.72	1.14 ± 0.06	0.00186	0.93	12.38 ± 0.16
EH2	65.55 ± 1.67	1.45 ± 0.09	0.00294	1.61	13.79 ± 0.16
EH3	55.13 ± 3.75	1.34 ± 0.12	0.00211	1.05	17.67 ± 0.18
EH4	60.12 ± 4.50	1.54 ± 0.04	0.00243	1.21	18.87 ± 0.30
EH5	70.59 ± 1.75	1.70 ± 0.03	0.00289	1.44	19.68 ± 0.45
EH6	78.56 ± 2.73	1.76 ± 0.04	0.00318	1.89	14.91 ± 0.19
EH7	75.47 ± 2.50	1.71 ± 0.01	0.00306	1.53	15.67 ± 0.20
EH8	85.17 ± 5.47	1.87 ± 0.04	0.00331	1.65	17.50 ± 0.15
EH9	124.78 ± 2.75	2.89 ± 0.03	0.00643	3.12	13.46 ± 0.45
B.Formulation (Cellulose 0.22 µm)					
EH1	40.40 ± 3.14	0.89 ± 0.03	0.00148	0.74	14.56 ± 0.37
EH2	45.49 ± 4.36	1.02 ± 0.12	0.00202	1.10	11.43 ± 0.53
EH3	44.13 ± 3.50	0.96 ± 0.18	0.00163	0.81	17.67 ± 0.37
EH4	48.31 ± 2.47	1.13 ± 0.05	0.00210	1.05	15.56 ± 0.39
EH5	55.13 ± 4.78	1.20 ± 2.47	0.00223	1.11	17.79 ± 0.15
EH6	68.75 ± 2.76	1.39 ± 0.16	0.00273	1.29	11.86 ± 0.19
EH7	75.12 ± 1.70	1.51 ± 0.13	0.00290	1.45	16.13 ± 0.28
EH8	86.50 ± 3.75	1.87 ± 0.04	0.00313	1.56	15.10 ± 0.10
EH9	106.69 ± 2.14	2.14 ± 0.08	0.00593	2.76	15.73 ± 0.34
Formulation (Nylon 0.22 µm)					
EH1	38.12 ± 2.57	0.61 ± 0.03	0.00153	0.76	11.67 ± 0.11
EH2	51.78 ± 1.89	1.19 ± 0.09	0.00216	1.08	12.83 ± 0.16
EH3	47.13 ± 4.50	0.96 ± 0.04	0.00198	0.99	15.78 ± 0.20
EH4	50.12 ± 3.56	1.14 ± 0.14	0.00203	1.01	16.12 ± 0.18
EH5	55.12 ± 1.27	1.32 ± 0.11	0.00275	1.37	18.10 ± 0.10
EH6	62.09 ± 2.45	1.56 ± 0.13	0.00284	1.42	14.94 ± 0.35
EH7	58.12 ± 1.78	1.42 ± 0.10	0.00238	1.19	19.37 ± 0.60
EH8	70.12 ± 4.50	1.66 ± 0.15	0.00274	1.37	17.68 ± 0.10
EH9	90.73 ± 3.17	1.97 ± 0.04	0.00519	2.49	16.65 ± 0.38

Data presented as mean ± standard deviation (SD), (n = 3)

studies showed that L-929 cells treated with compared to untreated cells had the same morphological changes. These same morphological conditions imply that the treatments with nano vesicular formulations did not undergo the apoptotic process, demonstrating their potent cytoprotective effects.

Live dead cell assay

The live dead cell assay distinguished cell vitality based on fluorescence staining. Live cells with intact membranes exhibited consistent green fluorescence with Syto-9, while dead cells with compromised membranes showed bright orange/

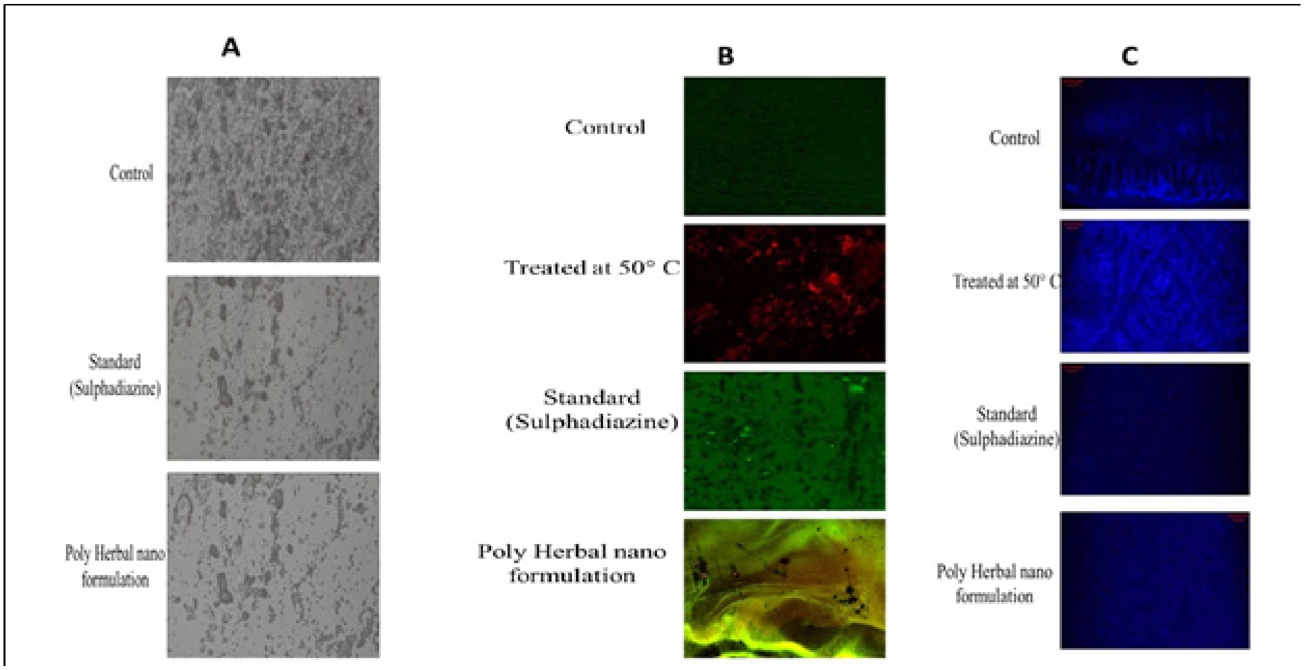

Figure 6: *In-vitro* studies of characterized ethosomes in (A) L-929 cell lines Cytotoxicity assay, (B) Live cell Proliferation Assay, (C) DAPI nucleic acid apoptotic assay

red fluorescence with propidium iodide. Application of EH2 polyherbal ethosomes to pre-treated burnt cells resulted in increased cell viability, evident by higher levels of dark orange-red fluorescence compared to control cells, showed in Figure 6 (B). This suggests ethosomes' protective and healing effects on the cell plasma membrane post-treatment.

DAPI Staining

The DAPI staining assay revealed the nuclear morphology of L-929 cells. Apoptotic cells typically exhibit nuclear alterations, including shrinkage, blebbing, chromatin condensation, nucleus fragmentation, and the formation of apoptotic bodies. DAPI, a blue fluorescent dye, was used to specifically bind to DNA and assess nuclear morphology changes indicative of apoptotic cell death. Both control and EH2 polyherbal ethosome-treated cells displayed no significant alterations in nuclear morphology or signs of apoptotic nuclear modifications, showed in Figure 6(C). The results indicate that treatment with polyherbal nano ethosomes did not induce apoptosis in L-929 cells (Figure 7).

Characterization and formulation of nanovesicular ethosomal gels

The physicochemical properties of the developed nanovesicular gel exhibited favorable characteristics, indicating its suitability for topical application. The gel displayed good homogeneity, and its color was observed to be yellow. The pH of the nanovesicular gel was measured at 5.78 ± 0.25, suggesting a neutral to a slightly acidic environment. Viscosity, a crucial factor in topical formulations, was found to be 368 ± 25.59 cPs, signifying an appropriate consistency for easy application. The spreadability of the gel, a key attribute influencing user experience, was determined to be 6.74 ± 1.29 gm cm/sec, indicating a formulation that can be readily spread on the skin. Extrudability, measured at 153 ± 0.57, further affirmed the ease with which the gel can be extruded. Collectively, these results highlight the successful development of a nanovesicular gel with desirable physiochemical properties, emphasizing its potential for effective and user-friendly topical use.

DISCUSSION

The quantitative analysis conducted in our study revealed notable disparities in the phytochemical composition of *P. paniculata, B. alba, P. oleraceae, L. inermis,* and *T. foenum* extracts compared to previous reports. Specifically, *P. paniculata* exhibited elevated levels of phenolic compounds and flavonoids in our investigation, contrasting with lower concentrations of alkaloids, phenols, tannins, and flavonoids reported.[19] This discrepancy may stem from differences

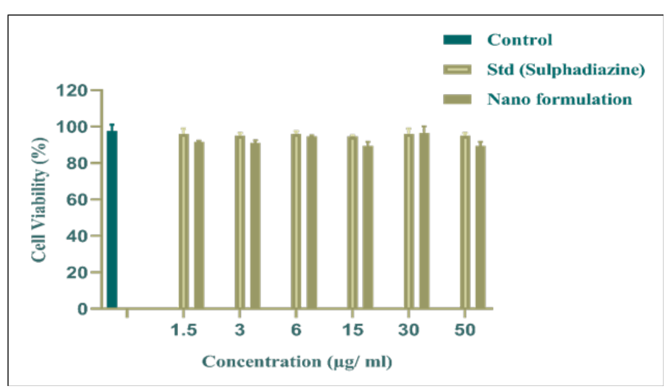

Figure 7: Percentage of cell viability of L929 cells

in plant material or extraction methodologies employed. Similarly, our study identified higher concentrations of tannin, flavonoid, phenolic, and alkaloid content in *B. alba* compared to percentages, suggesting potential variations in extraction techniques or plant sources reported.[20] Although our findings for *Lawsonia* extract indicated moderate levels of these compounds, A study reported substantially higher concentrations.[21] Nonetheless, our study underscores *Lawsonia*'s promising biocidal potential against termite attack and fungal decay, highlighting its significance in natural product research and environmental protection. Furthermore, our results demonstrated significantly higher levels of tannin, flavonoid, phenolic, and alkaloid content in *Trigonella* extract compared to that reported.[22] Despite methodological disparities, our findings emphasize *Trigonella*'s richness in these secondary metabolites, indicating its potential as a valuable natural resource.

The compounds identified in the extracts, particularly phenolic compounds, are well-acknowledged in cosmetic applications due to their redox activities and antioxidant attributes.[23] The higher phenolic content in the sample reinforces its antioxidant potential, aligning with previous studies emphasizing the role of phenols in determining redox activities. Additionally, flavonoids emerge as potent scavengers for oxidizing molecules and free radicals, being principal contributors to the antioxidant activities of plant materials.[24] The antimicrobial, anti-inflammatory, and antioxidant properties attributed to plants are associated with secondary metabolites such as tannins and flavonoids, with the hydroxyl group identified as a key functional component.[25] These findings underscore the importance of functional groups in determining physicochemical properties, aligning with the observations on entrapment efficiency, particle size, polydispersity index, and zeta potential in the study.[26]

Our study utilized FTIR analysis to comprehensively characterize the polyherbal extract, confirming the presence of essential functional groups, particularly emphasizing phenolic OH groups known for their medicinal properties. This compatibility observed between the plant extracts and selected excipients in pre-formulation studies provides a strong foundation for the synthesis of polyherbal nanoethosomes, suggesting their potential as advanced drug delivery systems.[23] The FTIR-confirmed presence of saponins, resins, tannins, flavonoids, and phenolic compounds in our analyzed plant extracts aligns well with prior research conducted.[27,28] These comprehensive findings contribute significantly to our understanding of the bioactive components and formulation considerations crucial for the development of polyherbal nanoethosomes, offering promising prospects for pharmaceutical applications. The study demonstrates that vesicles with a particle size below 300 nm have the capability to effectively deliver their payload to deeper layers of the skin. The vesicle size, as revealed in the investigation, is primarily influenced by varying concentrations of lipid and ethanol in the formulation.[29] Consistent with literature findings, maintaining a particle size smaller than 300 nm is crucial for optimal skin penetration. Increased ethanol concentration is associated with reduced membrane vesicle thickness, facilitating efficient penetration into deeper skin layers.[30] In assessing polydispersity index (PDI), values below 0.7 indicate a homogenous system with a narrow particle size distribution, aligning with the present study's criteria and emphasizing its potential for efficient skin delivery.[31]

In comparison to previous studies on epigallocatechin-3-gallate (EGCG), and polymeric nanoparticles targeting cancer cells while sparing healthy ones, our investigation into EH2 polyherbal nano formulation's effects on L929 cells revealed concentration-dependent cytotoxicity, indicating its potential cytotoxic activity against these cells.[32-34] Unlike the relatively nontoxic effects observed in healthy L929 cells with polymeric nanoparticles, EH2 formulation induced notable cytotoxic effects. However, the EH1 formulation also exhibited cytoprotective properties, preserving cell morphology and preventing apoptosis, contrasting with the apoptotic pathways targeted by polymeric nanoparticles in cancer cells. The live-dead cell assay confirmed EH2's ability to preserve cell plasma membranes, further supporting its cytoprotective effects. DAPI staining assay results were consistent with EH2 formulation not inducing apoptotic cell death in L929 cells, aligning with previous findings regarding polymeric nanoparticles. Overall, while EH2 formulation displayed cytotoxic activity against L929 cells, its cytoprotective effects suggest multifaceted therapeutic potential, warranting further investigation into its underlying mechanisms and clinical applications.

ACKNOWLEDGMENT

NIL

CONCLUSION

The polyherbal extract containing *Basella, Portulaca, Lawsonia*, *Trigonella, and Peristrophe* has shown promising potential in the healing of burn wounds. The FTIR analysis provided valuable insights into the chemical composition of the extract, while the Nanoethogel delivery system demonstrated its ability to effectively administer the extract to the wound site. Furthermore, the *in-vitro* studies using the mouse fibroblast cell line L-929, along with the DAPI staining and live dead cell assay, have illustrated the extract's positive impact on supporting the proliferation and viability of the fibroblast cells crucial for wound healing. Overall, the findings suggest that this polyherbal extract could be a valuable natural remedy for burn wound management. Further research and clinical trials are warranted to validate its efficacy and safety for potential therapeutic use. In addition, the optimization of the formulation and delivery system using Design Expert software could further enhance the efficacy and bioavailability of the polyherbal extract for burn wound healing. The use of Design Expert software for optimization can help determine the optimal ratios and concentrations of the individual herbal components in the polyherbal extract, as well as optimize the formulation parameters of the nanoethogel delivery system.

This would ultimately contribute to the development of a standardized and optimized product with improved therapeutic outcomes for burn wound patients.

REFERENCES

1. Soni H, Mishra K, Sharma S, Singhai AK. Characterization of Azadirachtin from ethanolic extract of leaves of Azadirachta indica. Journal of Pharmacy Research. 2012 Jan;5(1):199-201. DOI: https://www.cabidigitallibrary.org/doi/full/10.5555/20123162616
2. Menna C, Calista N, Aurino L, Dwijayanti AD. Aloe vera vs. Silver sulfadiazine for treating second–degree burn wounds: Evidence-based case report. International Journal of Applied Pharmaceutics. 2019;11:146-148. DOI: http://dx.doi.org/10.22159/ijap.2019.v11s6.33580
3. Gayathiri K, Chitra V. *In-vitro*, *In-vivo* Study of *Jatropha curcas* Leaves Extract, and Preparation of a Nanoemulsion by a Low-energy/Solvent-free Method, In-silico Study of β-Sitosterol in Ulcerative Colitis. International Journal of Drug Delivery Technology, 2024;14(1):265-273. DOI: 10.25258/ijddt.14.1.38
4. Martin P, Leibovich SJ. Inflammatory cells during wound repair: the good, the bad and the ugly. Trends in cell biology. 2005;15(11):599-607. DOI: https://doi.org/10.1016/j.tcb.2005.09.002
5. Pierce GF, Yanagihara D, Klopchin K, Danilenko DM, Hsu E, Kenney WC, Morris CF. Stimulation of all epithelial elements during skin regeneration by keratinocyte growth factor. The Journal of experimental medicine. 1994;179(3):831-840. DOI: https://doi.org/10.1084/jem.179.3.831
6. Gillis P, Savla U, Volpert OV, Jimenez B, Waters CM, Panos RJ, Bouck NP. Keratinocyte growth factor induces angiogenesis and protects endothelial barrier function. Journal of cell science. 1999;112(12):2049-2057. DOI: https://doi.org/10.1242/jcs.112.12.2049
7. Sun T, McMinn P, Coakley S, Holcombe M, Smallwood R, MacNeil S. An integrated systems biology approach to understanding the rules of keratinocyte colony formation. Journal of the Royal Society Interface. 2007;4(17):1077-1092. DOI: https://doi.org/10.1098/rsif.2007.0227
8. Obara K, Sumi K, Fukuda H. The use of multiple transcription starts causes the dual targeting of Arabidopsis putative monodehydroascorbate reductase to both mitochondria and chloroplasts. Plant and cell physiology. 2002;43(7):697-705. DOI: https://doi.org/10.1093/pcp/pcf103
9. Efferth T, Kahl S, Paulus K, Adams M, Rauh R, Boechzelt H, Hao X, Kaina B, Bauer R. Phytochemistry and pharmacogenomics of natural products derived from traditional Chinese medicine and Chinese materia medica with activity against tumor cells. Molecular Cancer Therapeutics. 2008;7(1):152-161. DOI: https://doi.org/10.1158/1535-7163.MCT-07-0073
10. Goswami M, Kulshreshtha M, Rao CV, Yadav S, Yadav S. Anti-ulcer potential of Lawsonia inermis L. leaves against gastric ulcers in rats. Journal of Applied Pharmaceutical Science. 2011:69-72. DOI: https://japsonline.com/abstract.php?article_id=23&sts=2
11. Raghav S Shraddha, Bhavna Kumar, Sethiya K Neeraj, Singhal Manmohan, Arya Swati. *In-vitro* Analysis of Antioxidant, Anti-inflammatory, Antidiabetic and Antimicrobial Studies of Kaempferol Ethosomes, International Journal of Drug Delivery Technology. 2024;14(1):118-125. DOI: 10.25258/ijddt.14.1.17
12. Hardy A, Poulos A, Emanuel N, Reed W. An investigation of advanced practice carried out by radiographers in New South Wales. Radiographer. 2010;57(3):29-33. DOI: https://doi.org/10.1002/j.2051-3909.2010.tb00134.x
13. Keenan LY, Muir C, Cuthbertson LM. Maximizing the benefit–minimizing the risk: the developing role of radiographers in performing intravenous injections. The British Journal of Radiology. 2001;74(884):684-689. DOI: https://doi.org/10.1259/bjr.74.884.740684
14. Azad AK, Wan Azizi WS, Babar ZM, Labu ZK, Zabin S. An overview of phytochemical, Anti-inflammatory and Antibacterial activity of *Basella alba* leaves extract. Middle-East Journal of Scientific Research. 2013;14(5):650-655. DOI: 10.5829/idosi.mejsr.2013.14.5.71225
15. Selvakumar S, Vimalanban S, Balakrishnan G. Quantitative determination of phytochemical constituents from Anisomeles malabarica. MOJ Bioequivalence Bioavailability. 2019;6(2):19-21. DOI: https://medcraveonline.com/MOJBB/MOJBB-06-00130.pdf
16. Pathan IB, Jaware BP, Shelke S, Ambekar W. Curcumin loaded ethosomes for transdermal application: Formulation, optimization, in-vitro and in-vivo study. Journal of Drug Delivery Science and Technology. 2018;44:49-57. DOI: https://doi.org/10.1016/j.jddst.2017.11.005
17. Panda S, Suryawanshi M. Fabrication, Characterization and Toxicity Evaluation Chemically Cross Linked Polymeric Material: A Proof of Concept. International Journal of Pharmaceutical Sciences and Nanotechnology (IJPSN). 2023;16(3):6522-6532. DOI: https://doi.org/10.37285/ijpsn.2023.16.3.6
18. Nayak D, Tawale RM, Aranjani JM, Tippavajhala VK. Formulation, Optimization and Evaluation of Novel Ultra-deforwsxmable Vesicular Drug Delivery System for an Antifungal Drug. AAPS PharmSciTech. 2020;21(5):1-10. DOI: https://doi.org/10.1208/s12249-020-01681-5
19. Shobana G, John NA, Rameshkannan N. Quantitative Analysis of Physicochemical and Phytochemical Constituents Medicinal Herbs. Journal of Stress Physiology & Biochemistry. 2023;19(3):79-86. DOI: https://cyberleninka.ru/article/n/quantitative-analysis-of-physicochemical-and-phytochemical-constituents-medicinal-herbs
20. Ibrahim TA, Ajongbolo KF, Aladekoyi G. Phytochemical Screening and Antimicrobial Activity of Crude Extracts of *Basella alba* and *Helianthus annuus* on Selected Food Pathogens. Research & Reviews: Journal of Microbiology and Biotechnology. 2014;3(2):27-31. DOI: https://www.semanticscholar.org/paper/Phytochemical-Screening-and-Antimicrobial-Activity-Ta-Kf/1f4d500488126b24d94cf9f410e11ee140492412
21. Adedeji GA, Ogunsanwo OY, Elufioye TO. Quantifications of phytochemicals and biocide actions of Lawsonia inermis linn. Extracts against wood termites and fungi. International Biodeterioration & Biodegradation. 2017;116:155-162. DOI: https://doi.org/10.1016/j.ibiod.2016.10.026
22. Mahmood NM, Yahya KI. Nutrient and phytochemical of fenugreek (Trigonella foenum graecum) seeds. International Journal of Sciences: Basic and Applied Research. 2017;36(3):203-213. DOI: http://gssrr.org/index.php?journal=JournalOfBasicAndApplied
23. Keser S, Celik S, Turkoglu S, Yilmaz O, Ismail T. Antioxidant activity, total phenolic and flavonoid content of water and ethanol extracts from Achillea millefolium L. Turkish Journal of Pharmaceutical Sciences. 2013;10(3):385–392. DOI: https://cms.galenos.com.tr/Uploads/Article_12377/385-392.pdf

24. Eghdami A, Sadeghi F. Determination of total phenolic and flavonoids contents in methanolic and aqueous extract of Achillea millefolium. Organic Chemistry Journal. 2010;2:81-84. DOI:https://api.semanticscholar.org/CorpusID:96668196
25. Kähkönen MP, Hopia AI, Vuorela HJ, Rauha JP, Pihlaja K, Kujala TS, Heinonen M. Antioxidant activity of plant extracts containing phenolic compounds. Journal of agricultural and food chemistry. 1999;47(10):3954-3962. DOI: https://pubs.acs.org/doi/abs/10.1021/JF990146L
26. Poojary MM, Passamonti P. Optimization of extraction of high purity all-trans-lycopene from tomato pulp waste. Food Chemistry. 2015;188:84-91. DOI: https://doi.org/10.1016/j.foodchem.2015.04.133
27. Liu F, Ng TB. Antioxidative and free radical scavenging activities of selected medicinal herbs. Life sciences. 2000;66(8):725-735. DOI: https://doi.org/10.1016/S0024-3205(99)00643-8
28. Muruganantham S, Anbalagan G, Ramamurthy N. FT-IR and SEM-EDS comparative analysis of medicinal plants, Eclipta alba Hassk and Eclipta prostrata Linn. Romanian Journal of Biophysics. 2009;19(4):285-294. DOI: https://www.rjb.ro/articles/259/smur.pdf
29. Sahu AR, Bothara SB. Formulation and evaluation of phytosome drug delivery system of boswellia serrata extract. International Journal of Research in Medical Sciences. 2015;4(2):94–99. DOI: 143746657719_Asit_20Sahu_20.pdf-libre.pdf
30. Ascenso A, Raposo S, Batista C, Cardoso P, Mendes T, Praça FG, Bentley MV, Simões S. Development, characterization, and skin delivery studies of related ultradeformable vesicles: transfersomes, ethosomes, and transethosomes. International journal of nanomedicine. 2015:5837-5851. DOI: https://www.tandfonline.com/doi/full/10.2147/IJN.S86186
31. Danaei MR, Dehghankhold M, Ataei S, Hasanzadeh Davarani F, Javanmard R, Dokhani A, Khorasani S, Mozafari MR. Impact of particle size and polydispersity index on the clinical applications of lipidic nanocarrier systems. Pharmaceutics. 2018;10(2):57. DOI: https://doi.org/10.3390/pharmaceutics10020057
32. Maya S, Sabitha M, Nair SV, Jayakumar R. Phytomedicine-loaded polymeric nanomedicines: potential cancer therapeutics. Multifaceted Development and Application of Biopolymers for Biology, Biomedicine and Nanotechnology. 2013:203-239. DOI: https://doi.org/10.1007/12_2012_195
33. Gnana RPM, Devhare LD, Dharmamoorthy G, Khairnar MV, Prasidha R. Synthesis, Characterisation, Molecular Docking Studies and Biological Evaluation of Novel Benzothiazole Derivatives as EGFR Inhibitors for Anti-breast Cancer Agents. International Journal of Pharmaceutical Quality Assurance. 2023;14(3):475-480. DOI: 10.25258/ijpqa.14.3.03
34. Priya MGR, Prasanth LML, Devhare LD, Yazdan SK, Gunjal S. Synthesis, DNA Binding, Molecular Docking and Anticancer Studies of Copper (II), Nickel (II), and Zinc (II) Complexes of Primaquine-based Ligand. International Journal of Pharmaceutical Quality Assurance. 2024;15(1):69-75. DOI: 10.25258/ijpqa.15.1.10